Superficies y Vacio **8**, 28-32(1999)

An interplay between the structure and giant magnetoresistance in laser treated Ag/Co multilayers

M. Jergel, Š. Luby, A. Anopchenko, E. Majková, M. Spasova
Institute of Physics of the Slovak Academy of Sciences, Dúbravská cesta 9, 842 28 Bratislava, Slovakia

V. Holý
Laboratory of Thin Films and Nanostructures, Masaryk University, Kotláøská 2, 611 37 Brno, Czech Republic

M. Brunel
Laboratoire de Cristallographie du CNRS, B.P.166, 38042 Grenoble Cedex 09, France

A.Luches, M. Martino
I.N.F.M. and University of Lecce, Department of Physics, 73100 Lecce, Ital

An interplay between the structure and giant magnetoresistance (GMR) evolution in Ag/Co multilayers exposed to excimer XeCl laser pulses with the fluences of (0.1-0.25) Jcm^{-2} for (1-200) times is studied. Two samples with different layer thickness ratios, Ag_4Co_1 and Ag_6Co_1, were electron-beam evaporated on Si(100) substrate. X-ray diffraction revealed polycrystalline face-centered cubic structure of the Ag layers which is strongly textured in Ag_4Co_1 multilayer while in other sample the layers are not structurally coherent. A strong texture in Ag_4Co_1 stabilizes the multilayer structure in the irradiation regime without melting and the GMR varies non-systematically in a rather narrow interval around the original value. Contrarily, the grain boundary diffusion of Ag into Co layers occurs due to laser treatment in Ag_6Co_1 leading to the formation of a discontinuous multilayer which enhances the GMR ratio more than twice. When the Ag melting threshold is reached, rapid solidification produces a granular-like structure irrespective of the structural character of the original multilayer and the GMR value changes unpredictably in a broad interval. The conclusions are supported by the hard X-ray reflectivity and diffuse scattering measurements as well as by transmission electron microscopy observations

.

I. Introduction

The giant magnetoresistance (GMR) effect in magnetic/non-magnetic multilayers (MLs) was discovered in 1988[1]. Magnetic moments in the magnetic layers separated by non-magnetic ones are coupled antiferromagnetically. The parallel alignment of magnetic moments achieved in an external magnetic field brings about a considerable decrease of the electrical resistance. The theoretical explanation of this effect is based mostly on the spin-dependent interface electron scattering[2].

A lot of effort has been devoted to an improvement of the GMR by a post-deposition annealing. The annealing-out of defects lowers the resistivity and enhances the GMR ratio while the interfaces may affect the GMR in different ways. A smoothening of interfaces due to the back diffusion may improve slightly the GMR in the first stages of annealing[3] while later the grain boundary diffusion leading to discontinuous magnetic layers increases the GMR considerably as it was shown for NiFeCo/Ag MLs[4]. As soon as the melting occurs, a recrystallized granular-like structure is formed without any correlation to the original structure. Consequently, the GMR may either increase or decrease considerably.

In this work, we report on the effect of pulsed excimer laser treatment on structure and the GMR of Ag/Co MLs. This type of heat treatment has been tried to modify the GMR for the first time only recently by us[5] though it has more advantages. It enables us to deposit a required amount of energy into the volume of a thin film without heating the substrate. This amount is controlled by two independent parameters – fluence and number of pulses.

II. Experimental

The samples were prepared by electron-beam evaporation onto Si(100) wafers covered by a 300 nm thick SiO_2. The vacuum prior and during the deposition was 10^{-7} Pa and 10^{-6} Pa, respectively. Two samples, nominally (4 nm Ag/1 nm Co)x10 and (6 nm Ag/1 nm Co)x5, were deposited starting with Ag. They are labeled further as Ag_4Co_1, Ag_6Co_1, respectively.

The thermal treatment was performed by excimer XeCl laser with a beam homogenizer in a vacuum of 10^{-3} Pa. The laser fluences were F=0.1, 0.15, 0.20, 0.25 Jcm^{-2}. The laser pulses were repeated n=1, 10, 20, 50, 100, 200 times with the frequency of 10 Hz, the pulse duration being 30 ns.

The structural analysis of the samples was performed by X-ray measurements using CuK_α radiation. The specular X-ray reflectivity (XRR) and diffuse scattering at grazing incidence were measured on a double-crystal high-resolution diffractometer where the $CuK_{\alpha 2}$ component was suppressed. The X-ray diffraction (XRD) was measured both in the symmetrical (Bragg-Brentano - BB) and asymmetrical (grazing incidence - GI) modes. The X-ray measurements were completed by the transmission electron microscopy (TEM) observations.

The electrical resistance $R(H)$ was measured as a function of the applied magnetic field up to 50 kOe at 4.2 K using a standard four probe method with Ag contacts.

Two geometries with magnetic field parallel or perpendicular to the sample surface were used. The GMR ratio was calculated as [*R*(*H*)-*R*(50kOe)]/*R*(50kOe). The magnetization measurements were performed using a SQUID magnetometer between 4.2 and 300 K.

As a direct measurement of the temperature in a laser irradiated sample is complicated due to very fast heating and cooling rates, numerical calculations were applied to find the temperature time and depth evolutions. The finite difference scheme as described in Ref. 6 was used. The calculations are valid for the first pulse only when the tabulated reflectivities may be applied. The surface temperature and depth of melting were determined for each fluence. For the fluences used and the repetition frequency of 10 Hz, the laser pulses are thermally independent Therefore the total deposited energy is proportional to the number of pulses for a given fluence. Both Co (T_{melt}=1768 K) and Ag (T_{melt}=1235 K) layers melt at the fluence F=0.25 Jcm^{-2} while Co layers remain solid for $F\leq$0.2 Jcm^{-2}. Ag layers melt at F=0.15 Jcm^{-2} for Ag_4Co_1 ML while for Ag_6Co_1 ML, they melt for the fluence F=0.25 Jcm^{-2} only. If Ag layers melt, they melt in the whole depth of MLs.

III. Results

The specular XRR curve of as-deposited Ag_4Co_1 ML as well as its evolution after F=0.15 Jcm^{-2} irradiation is shown in Fig.1. The most distinct maximum comes from the ML period (the 1st Bragg maximum) while the smaller ones are connected with the total thickness of the ML stack (so called Kiessig maxima). The existence of two kinds of maxima points to a rather regular ML structure in the as-deposited Ag_4Co_1 ML. It is not observed in other deposited ML because of a lower number of ML periods. At F=0.15 Jcm^{-2}, Ag_4Co_1 ML is heavily damaged for n=200. For F=0.1 Jcm^{-2} and n=200, Ag_4Co_1 ML is rather untouched. Ag_6Co_1 ML exhibits pronounced XRR modulations at F=0.15 Jcm^{-2} for all n as well as for F=0.2 Jcm^{-2} and n=20.

The XRR curves were simulated using the Fresnel optical computational code[7] to extract the basic ML parameters. 1 nm thick Co layers were supposed to be continuous according to Ref. 8. The evolution of ML parameters with laser treatment is documented in Table I. The parameter s called interface roughness was included into simulations by a Debye-Waller-like attenuation factor $\exp(-q_{j-1}q_j s^2)$ which modified the reflection coefficients of all interfaces, q_{j-1} and q_j being the scattering vectors above and below the jth interface, respectively. This attenuation factor corresponds to the error function interface profile of an interdiffused but flat interface or to a compositionally sharp but geometrically rough interface with Gaussian distribution of the deviations from a mean reference plane. These two extreme cases cannot be distinguished by a specular XRR measurement where the scattering vector is perpendicular to the interfaces.

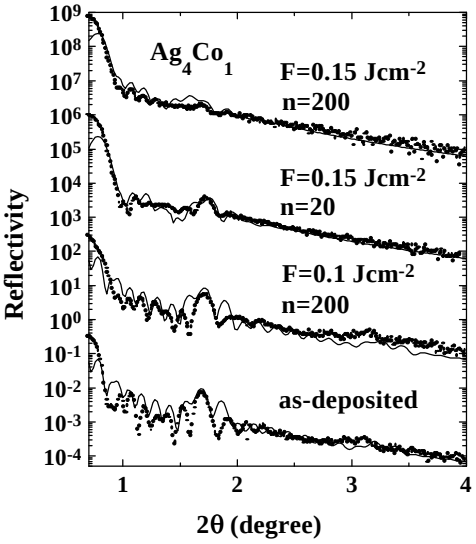

FIG. 1. Evolution of X-ray reflectivity with laser annealing forAg_4Co_1 ML. The measured curves (dots) were simulated by Fresnel optical computational code (line) and for laser treated samples they are shifted upwards. 2θ

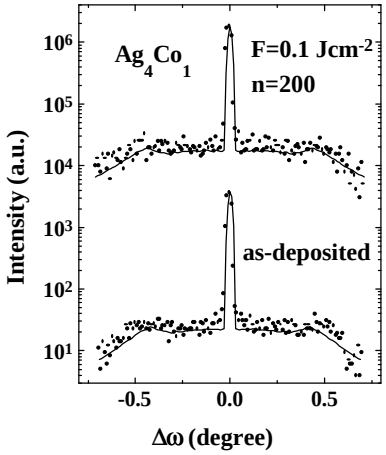

FIG. 2. Sample scans of Ag_4Co_1 ML before and after a laser treatment. The measured curves (dots) were simulated within distorted-wave Born approximation (line) and for laser treated samples they are shifted upwards. Δω means the offset from the specular position.

To characterize the interfaces completely, non-specular scans at grazing incidence with a non-zero lateral (along the interfaces) component of the scattering vector are unavoidable. We traced the distribution of the scattered intensity throughout the reciprocal space by sample (detector) scans at a fixed detector (sample) position. Some examples of the sample scans for the as-deposited and laser treated Ag_4Co_1 are shown in Fig.2. They are composed of a narrow central ridge and a broad background spanning nearly over the whole measured angular range. The central ridge is specular XRR broadened by the experimental resolution function and

TABLE I. Evolution of ML parameters with laser annealing obtained from the specular XRR simulations. *N, F, n, F_D, d, D, s* stand for the number of periods, fluence, number of pulses, deposited energy, individual layer thickness, ML period, and interface roughness, respectively. The layer thickness fluctuations included in the simulations reach 3-5 %.

sample	*N*	*F* [Jcm^{-2}]	*n*	F_D [Jcm^{-2}]	d_{Ag} [nm]	d_{Co} [nm]	*D* [nm]	*s* [nm]
Ag_4Co_1	10	0	0	0	4.7	1.1	5.8	0.6
		0.1	200	20	4.65	1.0	5.65	0.6
		0.15	10	1.5	4.4	1.1	5.5	1.0
			20	3	4.4	1.1	5.5	1.1
			200	30	3.5	1.8	5.3	1.8
Ag_6Co_1	5	0	0	0	5.5	1.2	6.7	1.1
		0.15	10	1.5	5.2	1.6	6.8	1.2
			50	7.5	4.65	2.0	6.65	1.3
			100	15	4.0	2.5	6.5	1.3

ML mosaicity while the broad background (diffuse scattering) is due solely to the real interface roughness. The diffuse scattering was simulated within the distorted-wave Born approximation (DWBA) to extract the parameters of the interface morphology and replication across the ML stack. The details of the calculations are described in Ref. 9. We used the Gaussian lateral (self) correlation function while the vertical replication of the interface profiles was included in the simulations by a vertical (cross) correlation function according to Ref. 10.

The internal structure of the layers was checked by the XRD measurements. The GI XRD patterns for Ag_6Co_1 ML taken at the angle of incidence α=0.5° is shown in Fig.3. It exhibits a complete set of diffraction maxima of the face-centered cubic (fcc) Ag phase. Moreover, the maximum labeled as I may point at the presence of small amount of close-packed hexagonal (hcp) Ag phase (203 diffraction). Co diffraction maxima are not seen due to the small thickness of Co layers and a low scattering power of Co atoms. Moreover, 200 diffraction of the fcc Ag phase partially overlaps with a strong 002 diffraction of the hcp Co phase (regular Co phase at room temperature). A trace of another diffraction of hcp Co, namely 200, is seen and labeled as II. The polycrystalline fcc Ag structure with random orientation of the grains persists after laser annealing at F=0.2 Jcm^{-2}. The BB XRD pattern of the as-deposited Ag_4Co_1 shows only 111 and 222 diffractions of fcc Ag. Moreover, the satellites around 111 diffraction are recognizable. These features hint at a strongly textured structure with (111) planes in Ag layers oriented preferentially parallel to the surface. From the positions of the satellites, the period of ≈5 nm is calculated corresponding to the ML period found from specular XRR. For F=0.1 Jcm^{-2}, the strongly textured structure is preserved up to n=200. For F=0.15 Jcm^{-2}, the texture is gradually lost with increasing n. The satellites disappear and another 200 diffraction of fcc Ag emerges from the background. For F=0.2 Jcm^{-2}, further diffractions appear. Some results of the GMR measurements are gathered in Table II. The GMR values are comparable with those reported in Ref. 8. The anisotropy of the GMR for perpendicular and parallel magnetic field was observed for all as-deposited and laser treated samples.

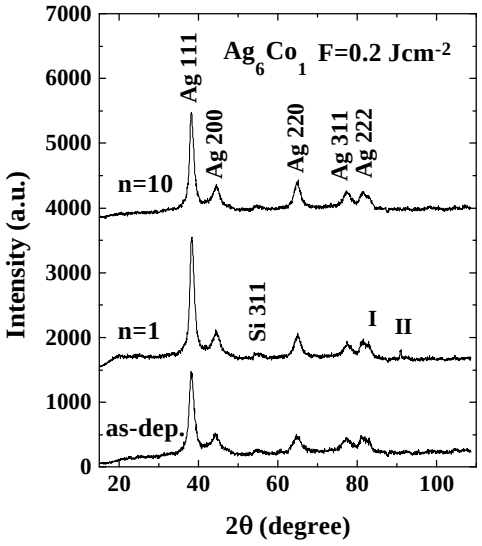

FIG. 3. X-ray diffraction patterns taken at grazing incidence of 0.5° before and after a laser treatment for Ag_6Co_1 ML. The curves for laser treated samples are shifted upwards. 2θ is the angle between the primary and secondary beams.

The changes of the GMR ratio for Ag_4Co_1 ML are not systematic but they are confined to a rather narrow interval around the original value. From F=0.2 Jcm^{-2}, when melting is in progress, the GMR changes increase. The specular XRR measurements hint at the formation of a more or less homogeneous thin film. For Ag_6Co_1 ML, the GMR increases systematically with the deposited energy in the irradiation regime without

TABLE II. Coercive field H_c, *GMR* ratio, and *DGMR/DH* with magnetic field in the film plane at 4.2 K for different fluences and number of pulses. For Ag_6Co_1 ML, the results for magnetic field perpendicular to the film plane are given in parentheses.

sample	F [Jcm^{-2}]	n	F_D [Jcm^{-2}]	H_c [Oe]	*GMR* [%]	*DGMR/DH* [%/Oe]
Ag_4Co_1	0	0	0	200	5.8	0.65
	0.1	1	0.1	300	6.3	0.45
		20	2	360	6.7	0.25
		200	20	310	5.3	0.47`
	0.15	1	0.15	260	4.7	0.53
		20	3	270	4.7	0.56
	0.2	1	0.2	390	1.26	---
Ag_6Co_1	0	0	0	430 (3900)	7.6 (7)	0.7
	0.1	10	1	345 (4200)	12.5 (11.7)	2.1
	0.15	10	1.5	360 (3500)	14 (12.8)	1.0
		100	15	430 (3900)	15 (15)	1.5
	0.2	20	4	330 (900)	13.5 (13.1)	1.0

melting, i.e. up to F=0.2 Jcm^{-2}. After F=0.15 Jcm^{-2} and n=100 irradiation, the GMR ratio is doubled for both orientations of magnetic field.

IV. Discussion

A high value of the GMR is determined by a large interfacial area between non-magnetic and magnetic components. The best conditions to fulfil this requirement are obviously in Ag_6Co_1 ML where a thermally driven process in the regime of laser irradiation without melting enhances gradually the GMR ratio. We suppose that this process takes place via grain boundary diffusion of Ag atoms into Co layers which start to be discontinuous. Such type of diffusion is favored because of immiscibility of Ag and Co. The formation of discontinuous MLs with enhanced GMR was reported for NiFe/Ag[11], FeCo/Ag[12], Co-Ag/Cu[13] and Co-Ag/Ag[14] MLs.

According to our recent studies of Co/Ag/Co trilayers[15], the diffusion coefficient of Ag in Co below 1000 K is 3x10^{-8} cm^{2}s^{-1}, the activation energy being only 0.38 eV. Such a low value of activation energy supports the concept of grain boundary diffusion. The diffusion lengths calculated for the above given value of the diffusion coefficient and for the pulse duration used are at the level of the Co layer thicknesses or larger for $n\geq 20$. This fact hints at the formation of discontinuous multilayer.

As it follows from the specular XRR simulations for Ag_6Co_1 MLs, the grain boundary diffusion of Ag atoms into Co layers is connected with a decrease of Ag layer thicknesses while opposite is the case for Co layers, the ML period being generally reduced. An enhanced refractive index of Co layers (by ≈10%), which had to be taken into account in the simulations, implies that these Co layers are in fact no more pure but "polluted" with Ag atoms penetrating between Co grains. When Ag layers start melting, one can assume a mixing of the liquid Ag/solid Co interfaces with a rapid solidification for each laser pulse. In the resulting granular-like structure, the GMR value is determined by number, sizes, shapes and distribution of Co clusters depending solely on the details of a highly non-equilibrium solidification process. A possible appearance of demagnetizing interparticle interactions has also to be taken into account[16].

As-deposited Ag_4Co_1 ML has smaller value of the GMR. An initial increase of the GMR ratio of Ag_4Co_1 ML for F=0.1 Jcm^{-2} and n=1 irradiation may be ascribed to the annealing-out of defects accompanied by a decrease of resistivity. Later, the GMR ratio changes non-systematically within an interval around the original value. The strong texture stabilizes the structure and prevents from the formation of a discontinuous ML via grain boundary diffusion promoting the GMR The layer thicknesses remain rather unchanged and the satellites around 111 diffraction of fcc Ag persist up to F=0.15 Jcm^{-2} and n=20 irradiation while the interface roughness increases. For n=200, Ag layers start melting and the GMR is unpredictably controlled by the granular-like structure formed.

As the interface roughness values determined from the specular XRR and diffuse scattering simulations are equal to each other ($s=s_r$) for all samples, the values of the interface roughness found from the specular XRR simulations are the real (geometrical) ones and are fully controlled by the grain morphology as may be expected owing to the immiscibility of Ag and Co. Therefore any change of the interface correlation, either lateral or

vertical one, is closely related to the grain morphology and size evolution induced by laser treatment. For Ag_6Co_1 ML, the vertical correlation length, comparable with the total ML thickness in as-deposited state, decreases at the level of Co layer thickness for F=0.15 Jcm^{-2} and n=50. This means that grain boundary diffusion breaks the replication of interface profiles completely. Simultaneously, the lateral correlation length decreases 5 times which hints at the formation of smaller grains in discontinuous ML which promotes the GMR ratio.

A small value of interface roughness in as-deposited Ag_4Co_1 ML is connected with its texture character resulting into ordered grains as observed by electron microscopy. Contrary to Ag_6Co_1 ML, the vertical and lateral correlation lengths of interface profiles are little affected by laser treatment and remain nearly the same for F=0.1 Jcm^{-2} and n=200 annealing. The interface roughness is also unchanged. For F=0.15 Jcm^{-2}, the interface roughness increases implying a small reorientation of the grains while the texture character of the ML structure is basically still preserved up to the melting threshold for Ag layers, as indicated by XRD measurements.

V. Conclusions

From the results presented it follows that the behavior of the GMR in Ag/Co MLs under study induced by laser irradiation is closely related to the underlying structural changes. For given irradiation conditions, these changes are determined by the structure of the layers in as-deposited state as well as by the ML design.

The best conditions for improving the GMR ratio are in Ag_6Co_1 ML with random polycrystalline structure inside the layers where the temperature window for grain boundary diffusion is broad enough to enable us to modify the GMR in a reasonable way. In Ag_4Co_1 ML, the structural coherence between the layers stabilizes the ML structure and prevents from the grain boundary diffusion and a consequent improving of the GMR ratio. The structural coherence is broken by melting Ag layers only. As soon as the melting threshold is reached, rapid solidification produces a granular-like structure irrespective of the structural character of the original ML and the GMR value changes unpredictably in a broad interval.

Acknowledgement

The authors acknowledge a partial support of the Slovak grant agency VEGA under grant no. 5083/98.

References

[1] M.N. Baibich, J. Brotto, A. Fert, F. Nguyen van Dau, F. Petroff, P. Etienne, G. Creuzet, A. Friedrich, and J. Chazelas, Phys. Rev. Lett. **61** 2472 (1988).
[2] R.E. Camley and J. Barnas, Phys. Rev. Lett. **63** 664 (1989).
[3] L.F. Shelp, G. Tosin, M.Carara, M.N. Baibich, A.A. Gomes, and J.E. Schmidt, Appl. Phys. Lett. **61** 1858 (1992).
[4] J.W. Dykes, Y.K. Kim, A. Tsoukatos, S. Gupta, and S.C. Sanders, J. Appl. Phys. **79** 5584 (1996).
[5] Š. Luby, E. Majková, M. Spasova, M. Jergel, R. Senderák, E. D'Anna, A.Luches, M. Martino, M. Brunel, and I.M.Dmitrenko, Thin Sol. Films **312** 15 (1998).
[6] E. D'Anna, S. Luby, A. Luches, E. Majkova, and M. Martino, Appl. Physics A **56** 429 (1993).
[7] J.H. Underwood and T.W. Barbee Jr., AIP Conf. Proc. **75** 170 (1981).
[8] R. Lolocc, P.A. Schroeder, W.P. Pratt, J. Bass, and A. Fert, Physica B **204** 274 (1995).
[9] M. Jergel, V. Holý, E. Majková, Š. Luby, R.Senderák, H.J.Stock, D.Menke, U.Kleineberg, and U.Heinzmann, Physica B **253** 28 (1998).
[10] Z.H. Ming, A. Krol, Y.L. Soo, H. Kao, J.S. Park, and K.L. Wang, Phys. Rev. B **47** 16373 (1993).
[11] T.R. Hylton, K.R. Coffey, M.A. Parker, and J.K. Howard, Science **161** 1021 (1993).
[12] J.D. Jarrat and J.A. Barnard, J. Appl. Phys. **79** 5606 (1996).
[13] M. Iijima, Y. Shimizu, N. Kojima, A. Tanaka, and K. Kobayashi, J. Appl. Phys. **79** 5602 (1996).
[14] Shi-Ming Zhou, Yu Wang,, Wei-Rong Zhu, Rong-Jun Zhang, Yu-Xiang Zheng, Quing-Yuan Jin, Liang-Yao Chen, Biao You, Wu Ji, An Hu, Hongru Zhai, and Honghi Shen, J. Appl. Phys. **83** 900 (1998).
[15] E. D.'Anna, G. Leggieri, A. Luches, M. Martino, G. Majni, G. Barucca, P. Mengucci, Š. Luby, E. Majková, and M. Jergel, Thin Sol. Films **343&344** 203 (1999).
[16] A.D.C. Viegas, J. Geshev, L.F. Shelp, and J.E. Schmidt, J. Appl. Phys. **82**
7058 (1997.